

1 **Impact of grids and dynamical cores in CESM2.2 on**
2 **the meteorology and climate of the Arctic**

3 **Adam R. Herrington** ¹, **Marcus Lofverstrom** ², **Peter H. Lauritzen** ¹ and
4 **Andrew Gettelman** ¹

5 ¹National Center for Atmospheric Research, 1850 Table Mesa Drive, Boulder, Colorado, USA
6 ²Department of Geosciences, University of Arizona, 1040 E. 4th Street, Tucson, AZ USA

7 **Key Points:**

- 8 • enter point 1 here
9 • enter point 2 here
10 • enter point 3 here

Abstract

[enter your Abstract here]

Plain Language Summary

[enter your Plain Language Summary here or delete this section]

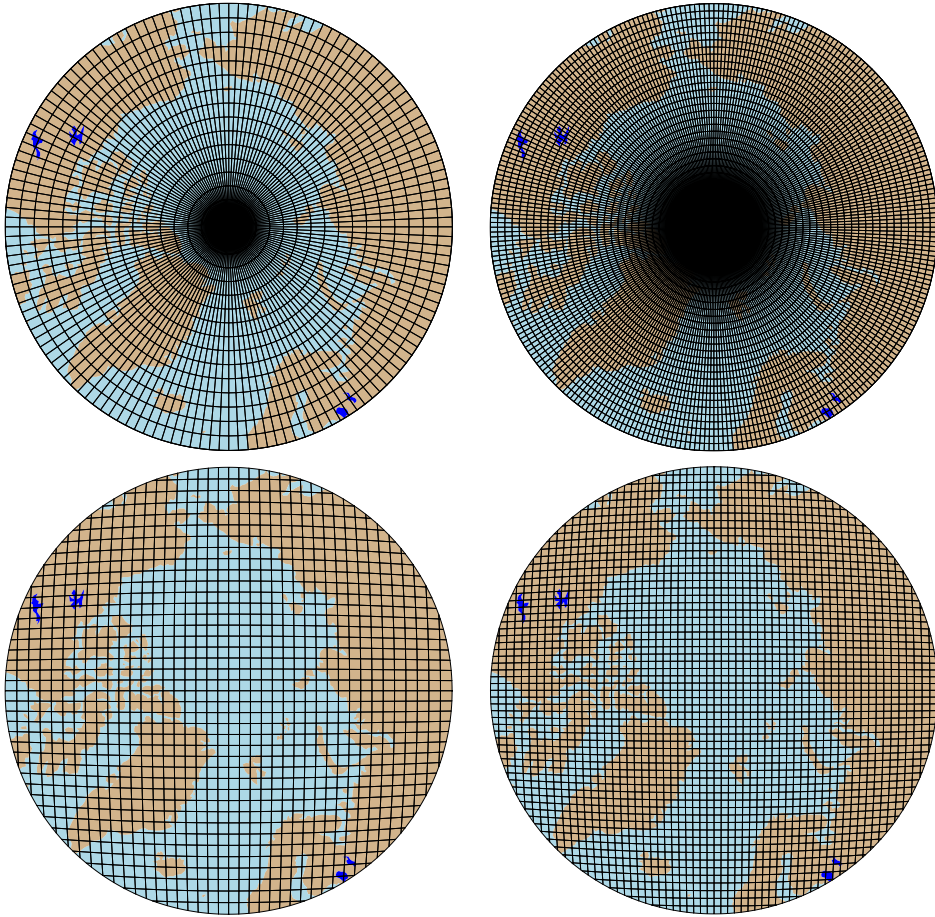
1 Introduction

General Circulation Models (GCMs) are powerful tools for understanding the meteorology and climate of the high-latitudes, which are among the most sensitive regions on Earth to global and environmental change. Despite their importance, the numerical treatment of polar regions is handled in vastly-different ways due to the so-called *pole-problem* (Williamson, 2007). The pole-problem refers to instability arising from the convergence of meridians at the polar points on latitude-longitude grids (e.g., Figure 1a). Depending on the numerics, methods exist to stabilize the pole problem, and latitude-longitude grids may be advantageous for polar processes as structures can be represented with more degrees of freedom than elsewhere in the computational domain. With the recent trend towards globally uniform unstructured grids, any potential benefits of latitude-longitude grids on polar regions may become a relic of the past. In this study, a spectrum of grids and dynamical cores (hereafter referred to as *dycores*) available in the Community Earth System Model, version 2.2 (CESM; <http://www.cesm.ucar.edu/models/cesm2/>), from conventional latitude-longitude grids to unstructured grids with globally uniform grid spacing to unstructured grids with regional refinement over the Arctic, are evaluated to understand their impacts on the simulated characteristics of the Arctic, with a special focus on the Greenland Ice Sheet.

In the 1970's the pole problem was largely defeated through wide-spread adoption of efficient spectral transform methods in GCMs. These methods transform grid point fields into a global, isotropic representation in wave space, where linear operators in the equation set can be solved for exactly. While spectral transform methods are still commonly used in the 21st century, local numerical methods have become desirable for their ability to run efficiently on massively parallel systems. The pole-problem has thus re-emerged in contemporary climate models that use latitude-longitude grids, and some combination of reduced grids and polar filters are necessary to ameliorate this instability (Jablonowski & Williamson, 2011). Polar filters are akin to a band-aid; they subdue the growth of unstable modes by applying additional damping to the solution over polar regions. One might expect that this additional damping reduces the effective resolution such that the resolved scales are similar across the entire domain, but this seems an unlikely and is explored further in this study.

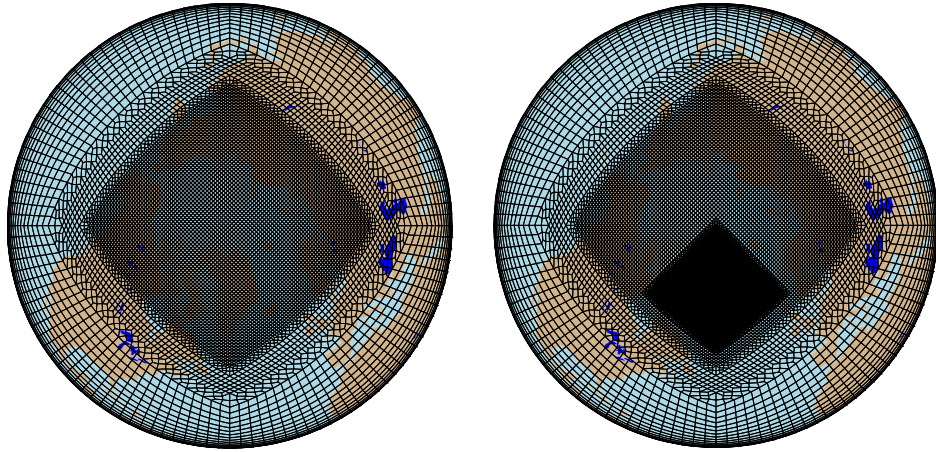
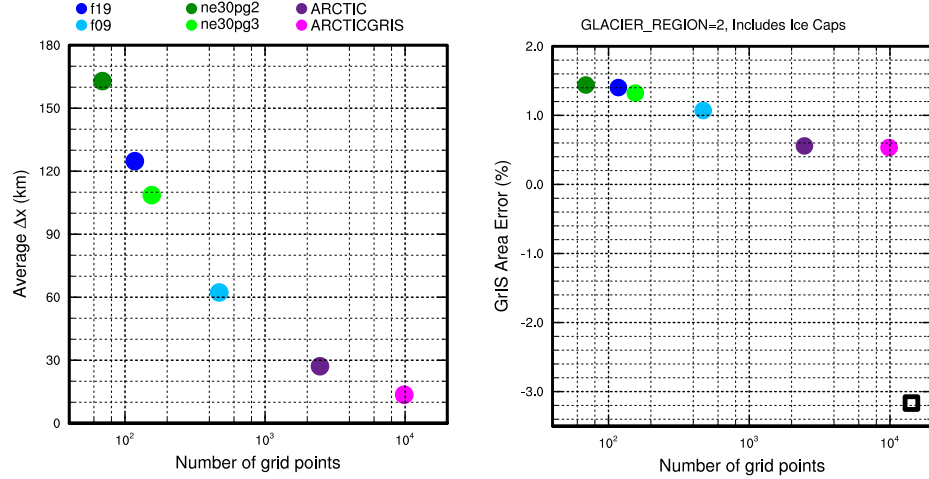
An alternative approach is to use unstructured grids. Unstructured grids allow for more flexible grid structures, permitting quasi-uniform grid spacing globally that eliminates the pole-problem entirely (e.g., Figure 1c). This grid flexibility also allows for variable-resolution or regional grid refinement. Grids can be developed with refinement over polar regions that could in principle make up for any loss in polar resolution in transitioning away from latitude-longitude grids (e.g., Figure 2), although this comes at the cost of a smaller CFL-limiting time-step in the refined region. But unstructured grids scale more efficiently on parallel systems than latitude-longitude grids, resulting in latitude-longitude grids becoming less common, and unstructured grids more common as computing power continued to increase over time.

The meteorology and climate of the Arctic is characterized by a range of processes and scales that are difficult to represent in GCMs (Bromwich et al., 2001; Smirnova & Golubkin, 2017; van Kampenhout et al., 2018). Synoptic scale storms are well represented

**Figure 1.** .

59 at typical GCM resolutions, but mesoscale Polar Lows are not. These mesoscale systems
 60 are prevalent during the cold season, and produce gale-force winds that can induce large
 61 fluxes through the underlying sea-ice/ocean interface. The Arctic also contains the Green-
 62 land Ice Sheet (hereafter denoted as *GrIS*). While it blankets the largest island in the
 63 world (Greenland), *GrIS* is only marginally resolved at typical GCM resolutions. *GrIS*
 64 ablation zones exert a primary control on the mass balance of the ice sheet, but are on
 65 the order of 100km wide, and models struggle to resolve these narrow features. *GrIS* el-
 66 evations descends rapidly toward the coasts, resulting in steep margins that facilitate oro-
 67 graphic precipitation events, but which are not well resolved in GCMs. The Arctic is there-
 68 fore well-suited to understand the impact of different grids and dycores on processes that
 69 are marginally resolved at conventional GCM resolutions.

70 The goal of this study is to characterize the representation of high-latitude regions
 71 using the spectral-element and finite-volume dycores in CESM2.2, as these models treat
 72 the high-latitudes, e.g., the pole-problem, in very different ways. The manuscript is laid
 73 out as follows. Section 2 consists of documentation of the grids, dycores and physical pa-
 74 rameterizations used in this study. The Arctic refined grids were developed by the au-
 75 thors, and this section serves as their official documentation in CESM2.2. Section 2 also
 76 contains a description of the experiments along with the observational datasets and post-
 77 processing software used for evaluating the models. Section 3 contains the results of the
 78 experiments and Section 4 provides some discussion and conclusions.

**Figure 2.****Figure 3.**

79 2 Methods

80 2.1 Dynamical cores

81 The atmospheric component of CESM2.2, the Community Atmosphere Model, ver-
 82 sion 6.3 (CAM; <https://ncar.github.io/CAM/doc/build/html/index.html>), supports
 83 a diverse number of atmospheric dynamical cores. These range from dycores using latitude-
 84 longitude grids, the finite-volume (FV; Lin, 2004) and eulerian spectral transform (EUL;
 85 Collins et al., 2006) models, and dycores built on unstructured grids, the spectral-element
 86 (SE; Lauritzen et al., 2018) and finite-volume 3 (FV3; Putman & Lin, 2007) models. The
 87 EUL dycore is the oldest dycore in CAM, and the least supported of all the dycores in
 88 the current model. FV3 is the newest dycore in CAM, but it was not fully incorporated
 89 at the time this work commenced, and so is omitted from this study. The authors instead
 90 focus on the two most well supported dycores in CAM, SE and FV.

91 **2.1.1 Finite-volume dynamical core**

92 The FV dycore is a hydrostatic model that integrates the equations of motion using
 93 a finite-volume discretization on a spherical latitude-longitude grid (Lin & Rood, 1997).
 94 The 2D dynamics evolve in floating Lagrangian layers that are periodically mapped to
 95 Eulerian reference grid in the vertical (Lin, 2004), using a hybrid-pressure vertical co-
 96 ordinate. Hyperviscous damping is applied to the divergent modes while Laplacian damp-
 97 ing is applied to momentum in the top few layers, referred to as a *sponge layer* (Lauritzen
 98 et al., 2011). A polar filter is used to avoid computational instability due to the conver-
 99 gence of the meridians, allowing for a more practical time-step. It takes the form of a
 100 Fourier filter in the zonal direction, with the damping coefficients increasing monoton-
 101 ically poleward (Suarez & Takacs, 1995).

102 **2.1.2 Spectral-element dynamical core**

103 The SE dycore is a hydrostatic model that integrates the equations of motion us-
 104 ing a high-order continuous Galerkin method (Taylor et al., 1997; Dennis et al., 2012;
 105 Lauritzen et al., 2018). The computational domain is a cubed-sphere grid tiled with quadri-
 106 lateral elements (e.g., Figure 2). Each element contains a fourth order basis set in the
 107 two horizontal directions, with the solution defined at the roots of the basis functions,
 108 the Gauss-Lobatto-Lagendre (GLL) quadrature points. This results in 16 GLL point val-
 109 ues within each element, with 12 of the points lying on the (shared) element boundary.
 110 Communication between elements happens via the direct stiffness summation (Canuto
 111 et al., 2007), which applies a numerical flux to the element boundaries to reconcile over-
 112 lapping nodal point values to produces a continuous global basis set.

113 As with the FV dycore, the dynamics evolve in floating Lagrangian layers that are
 114 subsequently mapped to a Eulerian reference grid. A dry mass vertical coordinate was
 115 more recently implemented for thermodynamic consistency with condensates (Lauritzen
 116 et al., 2018). The 2D dynamics have no implicit dissipation and so hyperviscosity op-
 117 erators are applied to all prognostic variables to remove spurious numerical errors (Dennis
 118 et al., 2012). Laplacian damping is applied in the sponge layer.

119 The SE dycore supports regional grid refinement via its variable-resolution config-
 120 uration, requiring two enhancements over uniform resolution grids. (1) As the numer-
 121 ical viscosity increases with resolution, explicit hyperviscosity relaxes according to the
 122 local element size, reducing their strength by about an order of magnitude per doubling
 123 of resolution. A tensor-hyperviscosity formulation is used (Guba et al., 2014), which ad-
 124 justs the coefficients in two orthogonal directions to more accurately target highly dis-
 125 torted quadrilateral elements. (2) The topography boundary conditions need to be smoothed
 126 in a way that does not excite grid scale modes. The NCAR topography software (Lauritzen
 127 et al., 2015) was modified to scale the smoothing radius by the local element size.

128 For spectral-element grids with quasi-uniform grid spacing, a variant in which tracer
 129 advection is computed using the Conservative Semi-Lagrangian Mulit-tracer tranport
 130 scheme is used instead (CSLAM; Lauritzen et al., 2017). CSLAM has improved tracer
 131 property preservation and accelerated multi-tracer transport. It uses a seperate grid from
 132 the spectral-element dynamics, through dividing each element into 3×3 quasi-equal area
 133 control volumes. The physical parameterizations are computed from the state on the CSLAM
 134 grid, which has clear advantages over the default SE dycore in which the physics are eval-
 135 uated at the GLL nodal points (A. Herrington et al., 2018).

136 **2.2 Grids**

137 Six grid are evaluated in this study (Table X). The FV dycore is run with 1° and
 138 2° grid spacing, referred to as *f09* and *f19*, respectively (Figure 1a,b). The 1° equiv-
 139 alent of the CAM-SE-CSLAM grid is also run, referred to as *ne30pg3* (Figure 1c), where

140 ne refers to a grid with of $ne \times ne$ elements per cubed-sphere face, and pg denotes that
 141 there are $pg \times pg$ control volumes per element for computing the physics. An additional
 142 1° CAM-SE-CSLAM grid is run, in which the physics are computed on a grid that is $\frac{3}{2} \times$
 143 larger than $pg3$ grid spacing, $ne30pg2$ (Figure 1d; A. R. Herrington et al., 2019).

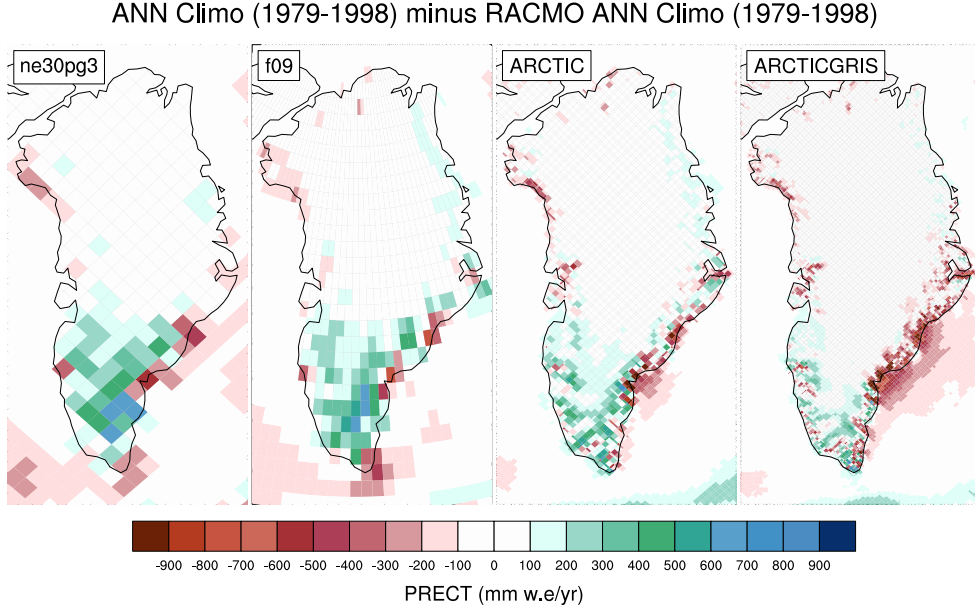
144 Two variable resolution meshes were developed as part of the CESM2.2 release that
 145 contains grid refinement over the Arctic. The software package SQuadgen (<https://github.com/ClimateGlobalChange/squadgen>) was used to generate these meshes. The *ARCTIC*
 146 grid is a 1° grid with $\frac{1}{4}^\circ$ regional refinement over the broader Arctic region. The *ARCTICGRIS*
 147 grid is identical to the *ARCTIC* grid, but contains an additional patch covering the big
 148 island of Greenland with $\frac{1}{8}^\circ$ resolution. Both of these grids are depicted in Figure 2.
 149

150 2.3 Physical parameterizations

151 The CAM6 physical parameterization package (hereafter referred to as the *physics*;
 152 <https://ncar.github.io/CAM/doc/build/html/index.html>) is used for all simula-
 153 tions in this study. CAM6 physics is most notably different from its predecessors through
 154 the incorporation of high-order turbulence closure, Cloud Layers Unified by Binormals
 155 (CLUBB; Golaz et al., 2002; Bogenschutz et al., 2013), which jointly acts as a PBL, shal-
 156 low convection and cloud macrophysics scheme. CLUBB is coupled with the MG2 mi-
 157 crophysics scheme (Gettelman et al., 2015), with prognostic precipitation and classical
 158 nucleation theory in representing cloud ice for improved cloud-aerosol interactions. Deep
 159 convection is parameterized using a convective quasi-equilibrium mass flux scheme (Zhang
 160 & McFarlane, 1995; Neale et al., 2008) including convective momentum transport (Richter
 161 et al., 2010). PBL form drag is modeled after (Beljaars et al., 2004) and orographic grav-
 162 ity wave drag is represented with an anisotropic method informed by the orientation of
 163 topographic ridges at the sub-grid scale.

164 2.4 Experimental design

165 All grids and dycores are run using an identical transient 1979-1998 AMIP-style
 166 configuration, with prescribed monthly SST/sea-ice after (Hurrell et al., 2008). This con-
 167 figuration refers to the *FHIST compset* and runs out of the box in CESM2.2. The Com-
 168 munity Land Model (CLM5; https://escomp.github.io/ctsm-docs/releases/clm5.0/html/users_guide/index.html), which uses the same grid as the atmosphere
 169 grid, calculates the surface energy balance at each land tile within a grid cell, which is
 170 used to compute snow and bare ice melting to inform the surface mass balance (SMB)
 171 of a glacier unit (van Kampenhout et al., 2020). Ice accumulation is modeled as a cap-
 172 ping flux, or snow in excess of the assumed 10 m snow cap, and refreezing of liquid within
 173 the snowpack additionally acts as a source of mass in the SMB calculation. Since the
 174 10 m snowcap needs to be reached in the accumulation zone to simulate the SMB, the
 175 snow depths in the variable-resolution grids were spun-up by forcing CLM5 offline, cy-
 176 cling over 20 years of a fully coupled *ARCTIC* run for about 500 years. The uniform
 177 resolution grids are all initialized with an SMB from an existing *f09* spun-up initial con-
 178 dition.
 179

**Figure 4.**

180 **2.5 Observational datasets**

181 **2.5.1 ERA5**

182 **2.5.2 LIVVkit 2.1**

183 **2.6 TempestExtremes**

184 **2.7 StormCompositor**

185 **3 Results**

186 **3.1 Tropospheric temperatures**

187 **3.2 Inter-annual variability**

188 **3.3 Synoptic-scale storm characteristics**

189 **3.4 Orographic gravity waves emanating from Greenland**

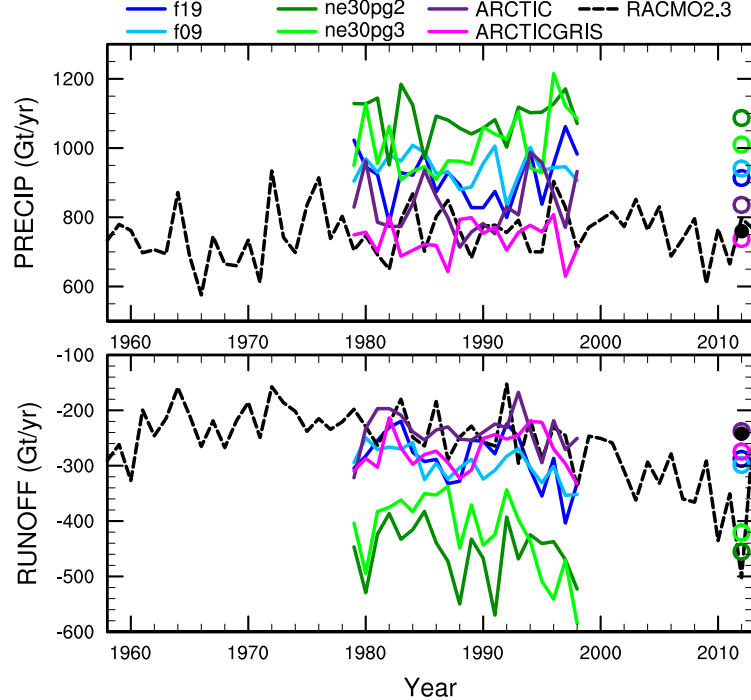
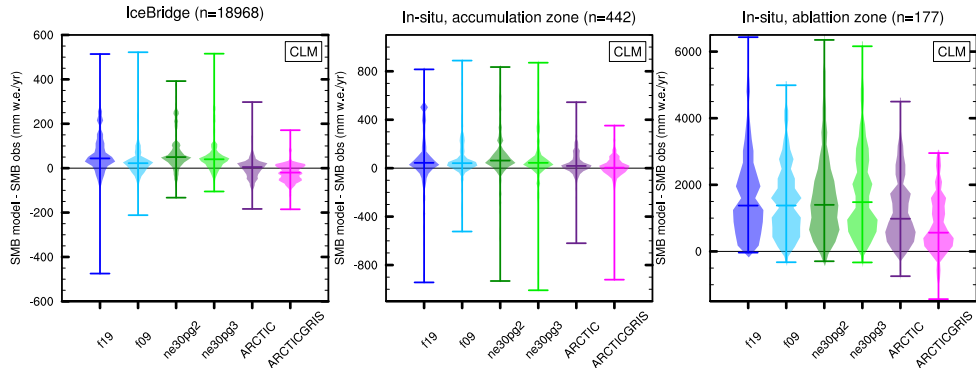
190 **3.5 Katabatic winds emanating from Greenland**

191 **3.6 Greenland surface mass balance**

192 **4 Conclusions**

193 **Acknowledgments**

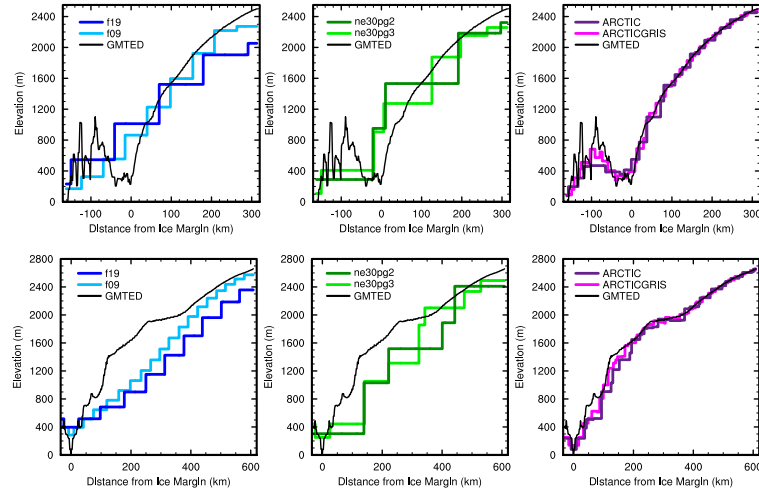
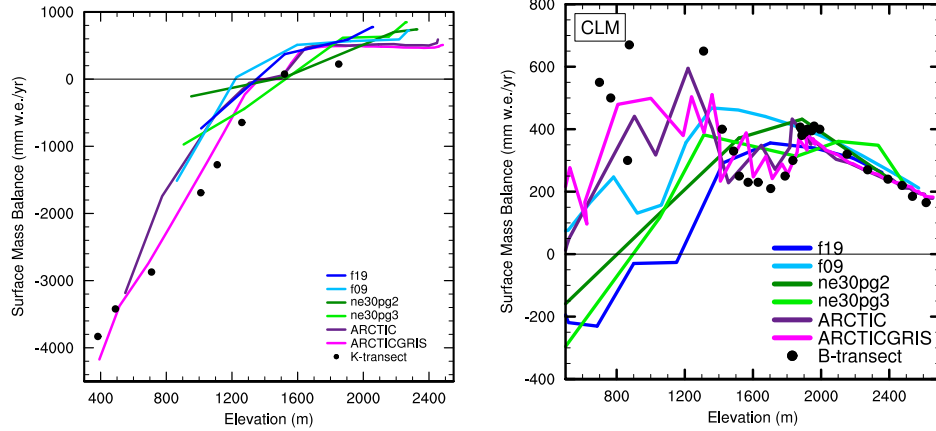
194 This material is based upon work supported by the National Center for Atmospheric Re-
 195 search (NCAR), which is a major facility sponsored by the NSF under Cooperative Agree-
 196 ment 1852977. Computing and data storage resources, including the Cheyenne super-
 197 computer (doi:10.5065/D6RX99HX), were provided by the Computational and Infor-
 198 mation Systems Laboratory (CISL) at NCAR.

**Figure 5.****Figure 6.**

199
200 The data presented in this manuscript is available at <https://github.com/adamrher/2020-arcticgrids>.

201 **References**

- 202 Beljaars, A., Brown, A., & Wood, N. (2004). A new parametrization of turbulent
203 orographic form drag. *Quart. J. Roy. Meteor. Soc.*, *130*(599), 1327–1347. doi:
204 10.1256/qj.03.73
- 205 Bogenschutz, P. A., Gettelman, A., Morrison, H., Larson, V. E., Craig, C., & Scha-
206 nen, D. P. (2013). Higher-order turbulence closure and its impact on climate
207 simulations in the community atmosphere model. *Journal of Climate*, *26*(23),
208 9655–9676.

**Figure 7.** .**Figure 8.** .

- 209 Bromwich, D. H., Cassano, J. J., Klein, T., Heinemann, G., Hines, K. M., Steffen,
 210 K., & Box, J. E. (2001). Mesoscale modeling of katabatic winds over greenland
 211 with the polar mm5. *Monthly Weather Review*, 129(9), 2290–2309.
- 212 Canuto, C., Hussaini, M. Y., Quarteroni, A., & Zang, T. (2007). *Spectral methods:*
 213 *Evolution to complex geometries and applications to fluid dynamics* (1st ed.).
 Springer.
- 214 Collins, W. D., Rasch, P. J., Boville, B. A., Hack, J. J., McCaa, J. R., Williamson,
 215 D. L., ... Zhang, M. (2006). The formulation and atmospheric simulation
 216 of the community atmosphere model version 3 (cam3). *Journal of Climate*,
 217 19(11), 2144–2161.
- 218 Dennis, J. M., Edwards, J., Evans, K. J., Guba, O., Lauritzen, P. H., Mirin, A. A.,
 219 ... Worley, P. H. (2012). CAM-SE: A scalable spectral element dynamical
 220 core for the Community Atmosphere Model. *Int. J. High. Perform. C.*, 26(1),
 221 74–89. Retrieved from <http://hpc.sagepub.com/content/26/1/74.abstract>
 222 doi: 10.1177/1094342011428142
- 223 Gettelman, A., Morrison, H., Santos, S., Bogenschutz, P., & Caldwell, P. (2015).
 Advanced two-moment bulk microphysics for global models. part ii: Global

- model solutions and aerosol–cloud interactions. *Journal of Climate*, 28(3), 1288–1307.
- Golaz, J.-C., Larson, V. E., & Cotton, W. R. (2002). A pdf-based model for boundary layer clouds. part i: Method and model description. *Journal of the Atmospheric Sciences*, 59(24), 3540–3551. doi: 10.1175/1520-0469(2002)059<3540:apbmfb>2.0.co;2
- Guba, O., Taylor, M. A., Ullrich, P. A., Overfelt, J. R., & Levy, M. N. (2014). The spectral element method (sem) on variable-resolution grids: evaluating grid sensitivity and resolution-aware numerical viscosity. *Geosci. Model Dev.*, 7(6), 2803–2816. doi: 10.5194/gmd-7-2803-2014
- Herrington, A., Lauritzen, P., Taylor, M. A., Goldhaber, S., Eaton, B. E., Bacmeister, J., ... Ullrich, P. (2018). Physics-dynamics coupling with element-based high-order galerkin methods: quasi equal-area physics grid. *Mon. Wea. Rev.*, 147, 69–84. doi: 10.1175/MWR-D-18-0136.1
- Herrington, A. R., Lauritzen, P. H., Reed, K. A., Goldhaber, S., & Eaton, B. E. (2019). Exploring a lower resolution physics grid in cam-se-cslam. *Journal of Advances in Modeling Earth Systems*, 11.
- Hurrell, J. W., Hack, J. J., Shea, D., Caron, J. M., & Rosinski, J. (2008). A new sea surface temperature and sea ice boundary dataset for the community atmosphere model. *Journal of Climate*, 21(19), 5145–5153.
- Jablonowski, C., & Williamson, D. L. (2011). The pros and cons of diffusion, filters and fixers in atmospheric general circulation models., in: P.H. Lauritzen, R.D. Nair, C. Jablonowski, M. Taylor (Eds.), Numerical techniques for global atmospheric models. *Lecture Notes in Computational Science and Engineering*, Springer, 80.
- Lauritzen, P. H., Bacmeister, J. T., Callaghan, P. F., & Taylor, M. A. (2015). Ncar global model topography generation software for unstructured grids. *Geoscientific Model Development Discussions*, 8(6), 4623–4651. doi: 10.5194/gmdd-8-4623-2015
- Lauritzen, P. H., Mirin, A., Truesdale, J., Raeder, K., Anderson, J., Bacmeister, J., & Neale, R. B. (2011). Implementation of new diffusion/filtering operators in the CAM-FV dynamical core. *Int. J. High Perform. Comput. Appl.*. doi: 10.1177/1094342011410088
- Lauritzen, P. H., Nair, R., Herrington, A., Callaghan, P., Goldhaber, S., Dennis, J., ... Dubos, T. (2018). NCAR CESM2.0 release of CAM-SE: A reformulation of the spectral-element dynamical core in dry-mass vertical coordinates with comprehensive treatment of condensates and energy. *J. Adv. Model. Earth Syst.*. doi: 10.1029/2017MS001257
- Lauritzen, P. H., Taylor, M. A., Overfelt, J., Ullrich, P. A., Nair, R. D., Goldhaber, S., & Kelly, R. (2017). CAM-SE-CSLAM: Consistent coupling of a conservative semi-lagrangian finite-volume method with spectral element dynamics. *Mon. Wea. Rev.*, 145(3), 833–855. doi: 10.1175/MWR-D-16-0258.1
- Lin, S.-J. (2004). A 'vertically Lagrangian' finite-volume dynamical core for global models. *Mon. Wea. Rev.*, 132, 2293–2307.
- Lin, S.-J., & Rood, R. B. (1997). An explicit flux-form semi-Lagrangian shallow-water model on the sphere. *Q.J.R.Meteorol.Soc.*, 123, 2477–2498.
- Neale, R. B., Richter, J. H., & Jochum, M. (2008). The impact of convection on ENSO: From a delayed oscillator to a series of events. *J. Climate*, 21, 5904–5924.
- Putman, W. M., & Lin, S.-J. (2007). Finite-volume transport on various cubed-sphere grids. *J. Comput. Phys.*, 227(1), 55–78.
- Richter, J. H., Sassi, F., & Garcia, R. R. (2010). Toward a physically based gravity wave source parameterization in a general circulation model. *J. Atmos. Sci.*, 67, 136–156. doi: dx.doi.org/10.1175/2009JAS3112.1
- Smirnova, J., & Golubkin, P. (2017). Comparing polar lows in atmospheric reanal-

- 281 yses: Arctic system reanalysis versus era-interim. *Monthly Weather Review*,
282 145(6), 2375–2383.
- 283 Suarez, M. J., & Takacs, L. L. (1995). Volume 5 documentation of the aries/geos dy-
284 namical core: Version 2.
- 285 Taylor, M. A., & Fournier, A. (2010). A compatible and conservative spectral el-
286 ement method on unstructured grids. *J. Comput. Phys.*, 229(17), 5879 - 5895.
287 doi: 10.1016/j.jcp.2010.04.008
- 288 Taylor, M. A., Tribbia, J., & Iskandarani, M. (1997). The spectral element method
289 for the shallow water equations on the sphere. *J. Comput. Phys.*, 130, 92-108.
- 290 van Kampenhout, L., Lenaerts, J. T., Lipscomb, W. H., Lhermitte, S., Noël, B.,
291 Vizcaíno, M., ... van den Broeke, M. R. (2020). Present-day greenland ice
292 sheet climate and surface mass balance in cesm2. *Journal of Geophysical*
293 *Research: Earth Surface*, 125(2), e2019JF005318.
- 294 van Kampenhout, L., Rhoades, A. M., Herrington, A. R., Zarzycki, C. M., Lenaerts,
295 J. T. M., Sacks, W. J., & van den Broeke, M. R. (2018). Regional grid refine-
296 ment in an earth system model: Impacts on the simulated greenland surface
297 mass balance. *The Cryosphere Discuss..* doi: 10.5194/tc-2018-257
- 298 Williamson, D. (2007). The evolution of dynamical cores for global atmospheric
299 models. *J. Meteor. Soc. Japan*, 85, 241-269.
- 300 Zhang, G., & McFarlane, N. (1995). Sensitivity of climate simulations to the pa-
301 rameterization of cumulus convection in the canadian climate centre general
302 circulation model. *Atmosphere-ocean*, 33(3), 407-446.